Seasonal to interannual variations in the intensity and central position of the surface Kuroshio east of Taiwan

Yi-Chia Hsin,[1] Bo Qiu,[2] Tzu-Ling Chiang,[3] and Chau-Ron Wu[3]

Received 26 February 2013; revised 15 July 2013; accepted 17 July 2013.

[1] Seasonal and interannual changes of surface Kuroshio intensity and central position east of Taiwan during 1993–2012 are investigated by quantitatively analyzing the satellite altimetry product. The Kuroshio moves inshore (offshore) off northeast of Taiwan in winter (summer), whereas it has an offshore (inshore) path off southeast of Taiwan in winter (summer). The seasonal change of heat flux over the East China Sea shelf is found to cause the seasonality of the Kuroshio central position off northeast of Taiwan, whereas the seasonal Kuroshio movement off southeast of Taiwan is found to be induced by the combined effect of the Kuroshio changes through the Luzon Strait and the eastern Luzon Island. In contrast to this y-dependent path changes, the Kuroshio becomes weaker (stronger) as a whole east of Taiwan in winter (summer). On the interannual time scales, the Kuroshio throughout the eastern coast of Taiwan intensifies and has a concurrent offshore path during the periods of 1995–1997 and 2004–2007. The relative intensity of cyclonic eddies to anticyclonic eddies off eastern Taiwan are found to contribute to these interannual Kuroshio changes.

Citation: Hsin, Y.-C., B. Qiu, T.-L. Chiang, and C.-R. Wu (2013), Seasonal to interannual variations in the intensity and central position of the surface Kuroshio east of Taiwan, *J. Geophys. Res. Oceans*, *118*, doi:10.1002/jgrc.20323.

1. Introduction

[2] The Kuroshio originates in the northern branch of the North Equatorial Current (NEC) and is one of the most important currents in the western Pacific. After bifurcating from the NEC off the Philippines, it passes by the Luzon Strait and continues flowing northward along the eastern coast of Taiwan. The Kuroshio enters the East China Sea (ECS) through the East Taiwan Channel (ETC, see Figure 1 for position). The Kuroshio east of Taiwan exerts a great impact on flows in the downstream regions of the ECS and south of Japan, and on water exchanges and biogeochemical processes in the ECS [*Chen*, 1996]. From in situ hydrographic surveys, current meter observations, and numerical models, the northward Kuroshio transport east of Taiwan is estimated to be about 30 Sv [see *Hsin et al*., 2008, Table 1]. On average, the width of Kuroshio spans from the east coast of Taiwan to 100–150 km offshore [*Liang et al*., 2003; *Hsin et al*., 2008] and its depth reaches down to 800–1000 m [*Hsin et al*., 2008].

[3] Variability of the Kuroshio ranging from days to years has been detected east of Taiwan [*Hsin et al*., 2008]. The Kuroshio south of the ETC is dominated by the intraseasonal time scale variations of 30–70 days and 100–200 days [*Johns et al*., 2001; *Hsin et al*., 2008, 2010]. The former variation is caused by Kuroshio's interaction with bottom topography, while the latter variation is due to the impinging of westward-propagating mesoscale eddies originating in the interior Pacific [*Yang et al*., 1999; *Qiu*, 1999; *Johns et al*., 2001; *Hwang et al*., 2004; *Hsin et al*., 2008, 2010, 2011]. *Johns et al*. [2001] suggested that the 100–200 day Kuroshio transport fluctuates at ±10 Sv during the period of September 1994 to May 1996.

[4] Seasonally, the Kuroshio northeast of Taiwan has been observed by most studies to be stronger in summer and weaker in winter [*Sun*, 1987; *Tang and Yang*, 1993; *Chuang and Liang*, 1994; *Ichikawa et al*., 2008; *Hsin et al*., 2011]. This seasonal change is mainly caused by the monsoon winds and heat flux over the shelf region [*Chao*, 1991; *Chuang and Liang*, 1994; *Oey et al*., 2010]. However, based on the 29 year tidal-gauge data, a different seasonal cycle of the Kuroshio, stronger in fall and weaker in spring, is proposed by *Chang and Oey* [2011] to be related to the seasonal eddy activity in the Subtropical Counter Current (STCC). The eddy kinetic energy in the STCC is larger in May and smaller in December [*Qiu*, 1999] and these eddies can alter the Kuroshio transport most effectively 4–6 months later. For the Kuroshio southeast of Taiwan, *Gilson and Roemmich* [2002] observed that the seasonal Kuroshio geostrophic transport is maximal in summer and minimal in winter based on 9 year expendable bathythermograph/expendable conductivity-temperature-depth data.

[1]Research Center for Environmental Changes, Academia Sinica, Taipei, Taiwan.
[2]Department of Oceanography, School of Ocean and Earth Science and Technology, University of Hawaii at Manoa, Honolulu, Hawaii, USA.
[3]Department of Earth Sciences, National Taiwan Normal University, Taipei, Taiwan.

Corresponding author: Y.-C. Hsin, Research Center for Environmental Changes, Academia Sinica, 128 Section 2, Academia Road, Nankang, Taipei 115, Taiwan. (ychsin@gate.sinica.edu.tw)

©2013. American Geophysical Union. All Rights Reserved.
2169-9275/13/10.1002/jgrc.20323

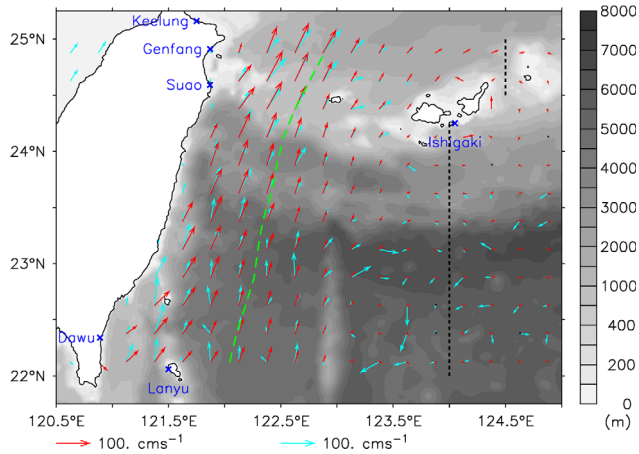

Figure 1. Annual mean Shipboard-Acoustic-Doppler-Profile (Sb-ADCP)-derived depth-averaged current (0–150 m) (light blue arrow) and AVISO-altimeter-based geostrophic current (red arrow) with bottom topography in gray shading. Green dashed curve denotes the mean altimeter-based Kuroshio central position (KCP). Sb-ADCP is compiled by the National Center for Ocean Research, Taiwan, using the observed data in the period of 1991–2005. Black dotted line shows the eastern limit for calculating KCP (X_E in equation (3)). The locations of six tidal-gauge stations are marked as blue crosses (x).

[5] On the interannual time scale, the Kuroshio variation east of Taiwan has been proposed to be related to the ENSO (El Niño and Southern Oscillation) index [e.g., *Hwang and Kao*, 2002] and the Pacific Decadal Oscillation (PDO) index [e.g., *Wu*, 2013]. *Gilson and Roemmich* [2002] suggested that the Kuroshio transport off southeast of Taiwan was larger in 1995 and 2000 and smaller in 1997–1998. *Hwang and Kao* [2002] proposed that the altimeter-based Kuroshio northeast of Taiwan has a positive correlation with ENSO with a 1 month lag and that the Kuroshio southeast of Taiwan has a negative correlation with ENSO with a 9–10 months lead. *Chang and Oey* [2011] also indicated that the Kuroshio strengthens in years of abundant eddies along the STCC. The level of eddy activities along the STCC modulates on interannual and decadal time scales in connection with the large-scale wind stress curl forcing that determines the eastward shear of the STCC [*Qiu and Chen*, 2010, 2013]. In addition, *Wu* [2013] suggested that, during the warm phase of the PDO, a southerly anomalous wind off the Philippines causes a northward shift of the NEC bifurcation latitude leading to a weakened Kuroshio transport southeast of Taiwan, and an abundant eddy activity in the STCC resulting in a strengthened Kuroshio transport off northeast of Taiwan. Besides, *Chang and Oey* [2012] related Kuroshio transport northeast of Taiwan to the oscillation of wind stress curls off eastern Taiwan and off eastern Philippines. They suggested that Kuroshio transport is increased due to the increased eddy activity dominated by warm eddies in the STCC in years when the wind stress curl off the eastern Philippines is larger than off eastern Taiwan.

[6] Although the seasonal fluctuation of the Kuroshio intensity (transport) east of Taiwan is smaller in amplitude compared to the fluctuations on intraseasonal and interannual time scales, it is nevertheless important to clarify the seasonality of the surface Kuroshio east of Taiwan and its connection to the prevailing seasonal surface wind and heat flux forcing around Taiwan. In the past studies, two different annual cycles of the Kuroshio intensity northeast of Taiwan have been proposed: summer versus winter (suggested by most studies) or fall versus spring (suggested by the recent study of *Chang and Oey* [2011]). The first goal of this study is to clarify the annual cycle of the surface Kuroshio intensity east of Taiwan, from both the altimetry and tidal-gauge (four stations northeast of Taiwan and two stations southeast of Taiwan) data. The second goal of this study is to detect the seasonality of the Kuroshio central position, a quantity that has not been examined before, with the use of satellite altimeter data. Third, interannual changes in the intensity of the surface Kuroshio east of Taiwan will be reexamined, and those of the surface Kuroshio central position will be explored for the first time. In section 2, we will describe the data and dynamic properties adopted in this study. Results and discussions are provided in section 3, and conclusions are summarized in the final section.

2. Data and Quantities

2.1. Satellite Altimetry Data

[7] The satellite altimeter sea surface height anomaly (SSHA) data are provided by AVISO (Archiving, Validation and Interpretation of Satellite Oceanographic data, http://www.aviso.oceanobs.com/), which is merged from multisatellite altimeter data of the TOPEX/Poseidon, ERS-1&2 (European Remote Sensing satellite 1&2), Jason-1&2, Envisat, and GFO (Geosat Follow On) missions. The product is gridded on a Mercator grid of 1/3° × 1/3° and a time interval of 1 day. It is available after October 1992. By adding the mean dynamic topography of *Rio et al.* [2011] to SSHA, we obtain the absolute sea surface height (SSH).

[8] Based on the geostrophic balance, the surface geostrophic velocities are calculated from the absolute SSH as follows.

$$U_g(x,y,t) = -\frac{g}{f(y)}\frac{\partial h(x,y,t)}{\partial y}, \quad (1)$$

$$V_g(x,y,t) = -\frac{g}{f(y)}\frac{\partial h(x,y,t)}{\partial x}, \quad (2)$$

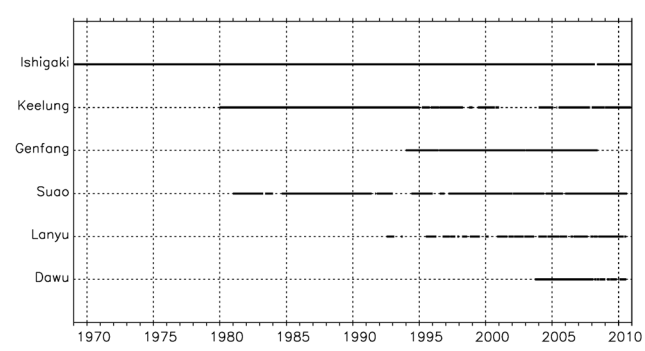

Figure 2. Executed duration of data available at the six tidal-gauge stations.

where x, y, and t are longitude, latitude, and time, respectively, U_g and V_g are the zonal and meridional components of the geostrophic current, respectively, h is the absolute SSH, g is the gravitational acceleration, $f(y) = 2\Omega\sin(y)$ is the Coriolis parameter, and Ω is the angular velocity of the Earth's rotation. SSH and geostrophic current data between January 1993 and December 2012 are utilized in this study.

2.2. Sea Level Records at Tidal-Gauge Stations

[9] Sea level data recorded at six tidal-gauge stations around Taiwan are used in this study for comparing the variability of the Kuroshio intensity with that derived from the altimetry data. As shown in Figure 1, four stations (Ishigaki, Keelung, Genfang, and Suao) are located around the northeastern Taiwan and two (Dawu and Lanyu) are located around the southeastern Taiwan. Except for the hourly sea level record at Ishigaki being downloaded from the University of Hawaii Sea Level Center (UHSLC, http://uhslc.soest.hawaii.edu), the hourly data at the other five stations are provided by the Central Weather Bureau, Taiwan (http://www.cwb.gov.tw/eng/index.htm). Durations of sea level record available at each station are shown in Figure 2. The hourly sea level data are averaged to the monthly interval by the following steps. First, obvious errors are corrected and gaps less than 25 h are interpolated linearly. Second, the hourly data are averaged daily when the number of data in a day is greater than 12. The monthly data are then averaged from the daily data when the number of data in a month is greater than 15. Finally, the monthly SSHA data at each station are derived by subtracting the mean sea level averaged over the entire period of the station shown in Figure 2.

2.3. Kuroshio Central Position

[10] In order to quantify the variation of Kuroshio path east of Taiwan, a quantity, based on the concept of center of mass, is defined as follows.

$$\mathrm{KCP}(y,t) = -\frac{\int_{X_W}^{X_E} x \cdot \mathrm{RV_g}(x,y,t)dx}{\int_{X_W}^{X_E} \mathrm{RV_g}(x,y,t)dx}, \tag{3}$$

where KCP is the Kuroshio Central Position, X_E and X_W are the eastern and western integral limits, and RV_g is the rotated V_g at an angle of 70°, which in general follows the direction of the eastern coastline of Taiwan. In equation (3), X_W follows the eastern coastline of Taiwan, and X_E is set to 123.75°E in the region south of 24.25°N and 124.25°E in the region north of 24.25°N (the black dotted line in Figure 1). The choice of the eastern integral limit is according to the eastern boundary of mean flow pattern east of Taiwan (arrows in Figure 1). Because the Kuroshio is thought of as a northward-flowing current, RV_g is set to zero for the negative V_g.

2.4. Kuroshio Intensity

[11] The Kuroshio intensity can be expressed by both the altimeter-derived geostrophic velocity and the tidal-gauge-derived SSHA. Based on tidal-gauge records, the Kuroshio intensity (INT_{TG}) can be expressed by the difference of SSHA between a station along the Taiwan coast and an offshore island station east of Taiwan [*Yang et al.*, 2001; *Chang and Oey*, 2011; *Hsin et al.*, 2011]:

$$\mathrm{INT_{TG}} = \mathrm{SSHA_E} - \mathrm{SSHA_W}, \tag{4}$$

where $SSHA_W$ is the SSHA at the tidal-gauge station along the Taiwan coast and $SSHA_E$ is the SSHA at the island tidal-gauge station (i.e., Ishigaki or Lanyu).

[12] By means of surface geostrophic velocity, the surface Kuroshio intensity (INT_{Vg}) can be calculated by:

$$\mathrm{INT_{V_g}} = \int_{X_W}^{X_E} \mathrm{RV_g}(x,y,t)dx, \tag{5}$$

where X_W and RV_g have the same definitions as those in equation (3); however, the eastern integral limit, X_E, is set to 124°E in the ETC (24.25–24.75°N) and is set to KCP + 1° at other latitudes. The 1° band is chosen because the eastern boundary of mean Kuroshio is roughly located at 1° east of the central position (Figure 1). Changing the band width affects only the magnitude of the calculated Kuroshio intensity, not its temporal signals. This method for estimating the intensity of a surface current was used in *Hsin and Qiu* [2012], who investigated the strength changes of the eastward-flowing Pacific North Equatorial Countercurrent following its eastward pathway.

3. Results and Discussions

3.1. Mean State of the Surface Kuroshio East of Taiwan

[13] The 20 year (1993–2012) mean altimeter-based geostrophic current is shown in Figure 1. The mean surface Kuroshio has two cores southeast of Taiwan and merges into one north of about 23°N. It has a maximum geostrophic velocity of about 1 ms^{-1} near 24°N and covers a width of about 2°. In terms of the magnitude and flow direction, the altimeter-based geostrophic current corresponds favorably to the depth-averaged current derived from the shipboard Acoustic Doppler Current Profilers (Sb-ADCP, light-blue arrow in Figure 1) and the numerical simulated surface flow [*Hsin et al.*, 2008].

[14] With the use of equations (3) and (5), the daily KCP and INT_{Vg} between 22 and 25°N east of Taiwan are calculated for the period of 1993–2012. Based on the 20 year data, Figure 3 shows the latitude-dependent mean and standard deviation of KCP and INT_{Vg}. The mean KCP is located at about 122.1°E southeast of Taiwan and at about 122.9°E northeast of Taiwan, following in general the eastern coastline of Taiwan (green dashed line in Figures 1 and 3a). The mean Kuroshio is closest to the Taiwan coast in the middle section and farthest away in the southern section (Figure 1). The variability of KCP is smaller around the ETC due to the confinement of Kuroshio by the ETC and is larger south and north (Figure 3b). The largest variability of KCP occurs in the area south of 23°N.

[15] As revealed in Figures 3c and 3d, the intensity of surface Kuroshio is weaker (stronger) in the southern (northern) section with a larger (smaller) variability. This larger variability south of the ETC is likely due to the impinging of mesoscale eddies originated in the STCC

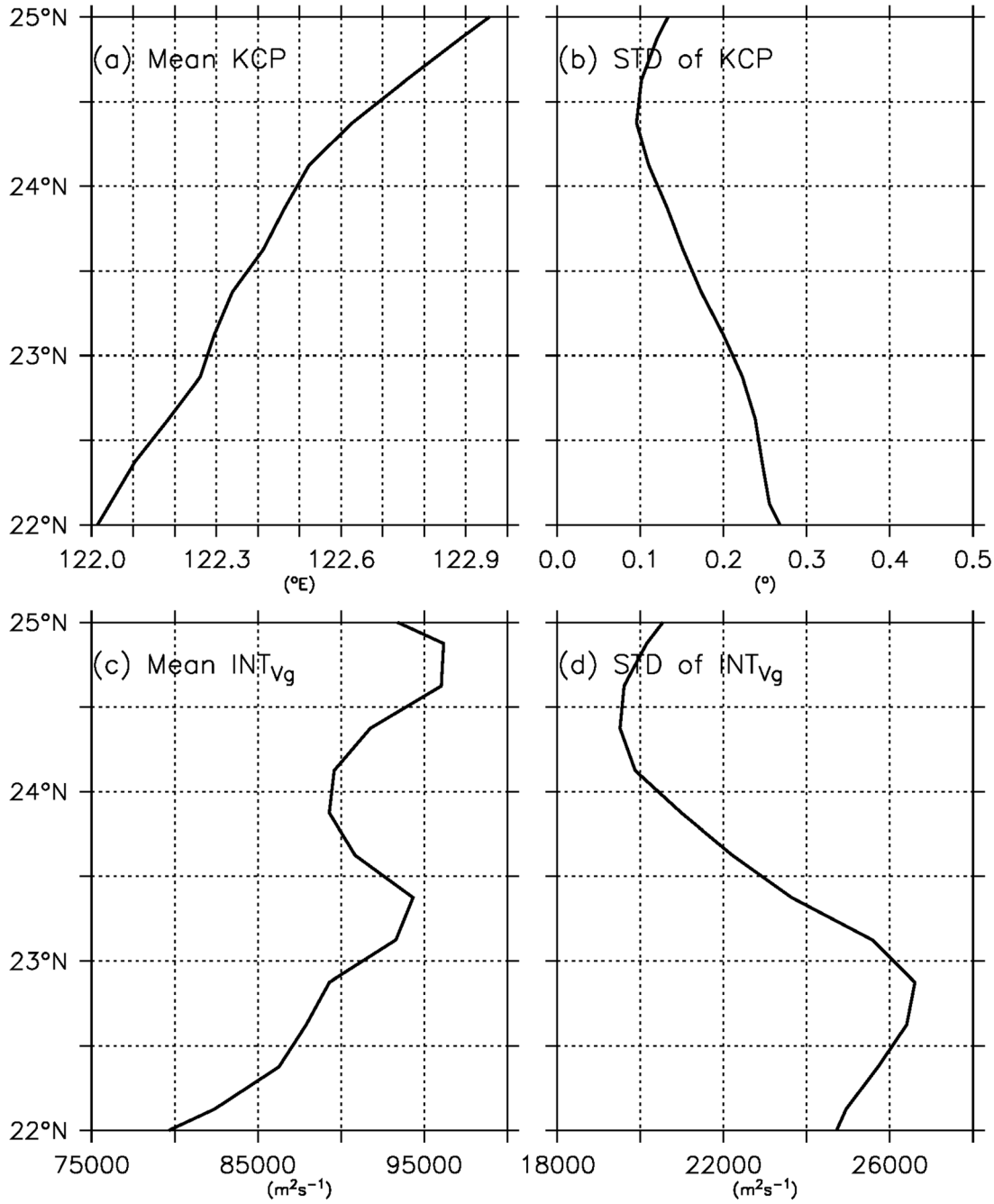

Figure 3. Latitude-dependent (a and c) mean and (b and d) standard deviation of altimeter-based central position (KCP) and intensity (INT_{Vg}) of the Kuroshio between 22 and 25°N east of Taiwan. Mean and standard deviation are derived from the data in the period between January 1993 and December 2012. The mean KCP in Figure 3a is the same as the green dashed line in Figure 1.

[*Johns et al*., 2001; *Hsin et al*., 2008, 2011]. It is noteworthy that the increasing Kuroshio intensity toward the north derived from the altimetry geostrophic velocity differs from the Sb-ADCP-based depth-integrated transport (0–300 m), which has a decreasing tendency toward the north, as suggested by *Liang et al*. [2003]. This difference could be due to the fact that the sea level change observed by the satellite altimeters reflects the change of the thermocline interface in the subsurface, or due to the eastward turning of the Kuroshio northeast of Taiwan. This notion is supported by the transport calculation from the model simulation by *Hsin et al*. [2008]. Their results showed that the meridional distribution of simulated transport is similar to that of the Sb-ADCP-based transport when the depth of 300 m is adopted as the lower integration limit, whereas the distribution is similar to that of the altimeter-derived Kuroshio intensity when the depth of 800 m, the bottom of Kuroshio, is chosen. Therefore, the northward increase in the Kuroshio transport could result from the deepening of the Kuroshio toward the north or the enhancement of

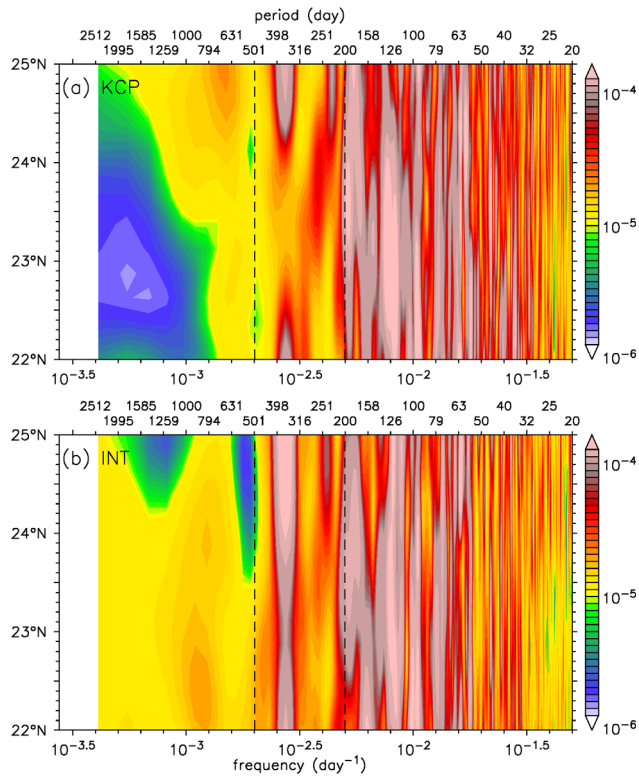

Figure 4. Latitude-dependent spectra of normalized Kuroshio (a) central position and (b) intensity. The central position and intensity are normalized by the latitude-dependent standard deviation as shown in Figures 3b and 3d, respectively. Vertical dashed lines represent the periods of 200 and 500 days. Both spectra are smoothed by a 5-point Hanning window.

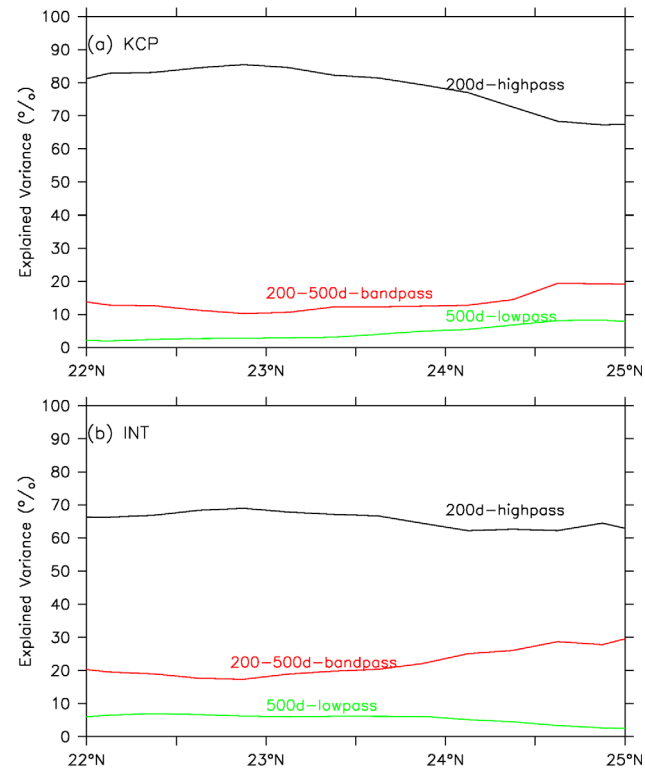

Figure 5. Latitude-dependent explained variances of 200 day high pass (black), 200–500 day band pass (red), and 500 day low pass (green) filtered (a) central position and (b) intensity of the Kuroshio.

recirculating flow in the area south of the ETC [*Hsin et al.*, 2008].

3.2. Variability of the Surface Kuroshio on Different Time Scales

[16] Utilizing the Fast Fourier Transform, spectral analyses are presented in Figure 4 to describe the variability of KCP and INT_{Vg}. For both the KCP and INT_{Vg}, dominant variations are found on time scales at 1 year and shorter than 200 days. On the interannual time scales (>500 days), however, the KCP and INT_{Vg} show different spectral distributions. The interannual fluctuations for the KCP are stronger in the northern section, whereas those for the INT_{Vg} are slightly stronger in the southern section.

[17] To further examine the contribution of the fluctuations in different periods, we plot in Figure 5 the explained variances of 200 day high pass filtered (intraseasonal), 200–500 day band pass filtered (seasonal), and 500 day low pass filtered (interannual) Kuroshio central position and intensity signals as a function of latitude. The intraseasonal fluctuations dominate both the KCP and INT_{Vg}. It explains over 60% of the total variance with a larger explained variance (>80%) in the south of the ETC, where the Kuroshio is not sheltered by islands to the east. The secondary signal is the seasonal one (200–500 day band pass filtered) which accounts for about 10–20% with a smaller value in the south of the ETC, where the explained variance is largely

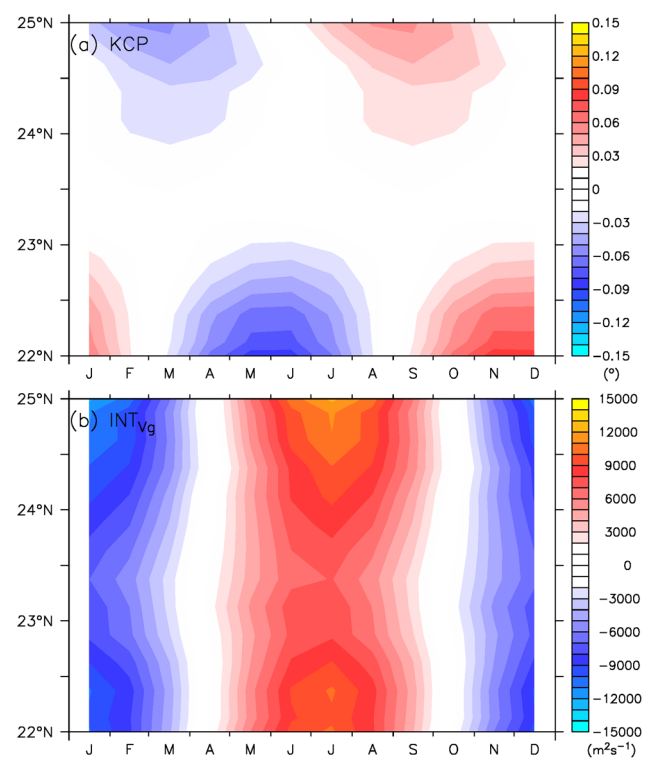

Figure 6. Monthly climatology of latitude-dependent anomalies of Kuroshio (a) central position and (b) intensity east of Taiwan compiled from the 200–500 day band pass filtered time series.

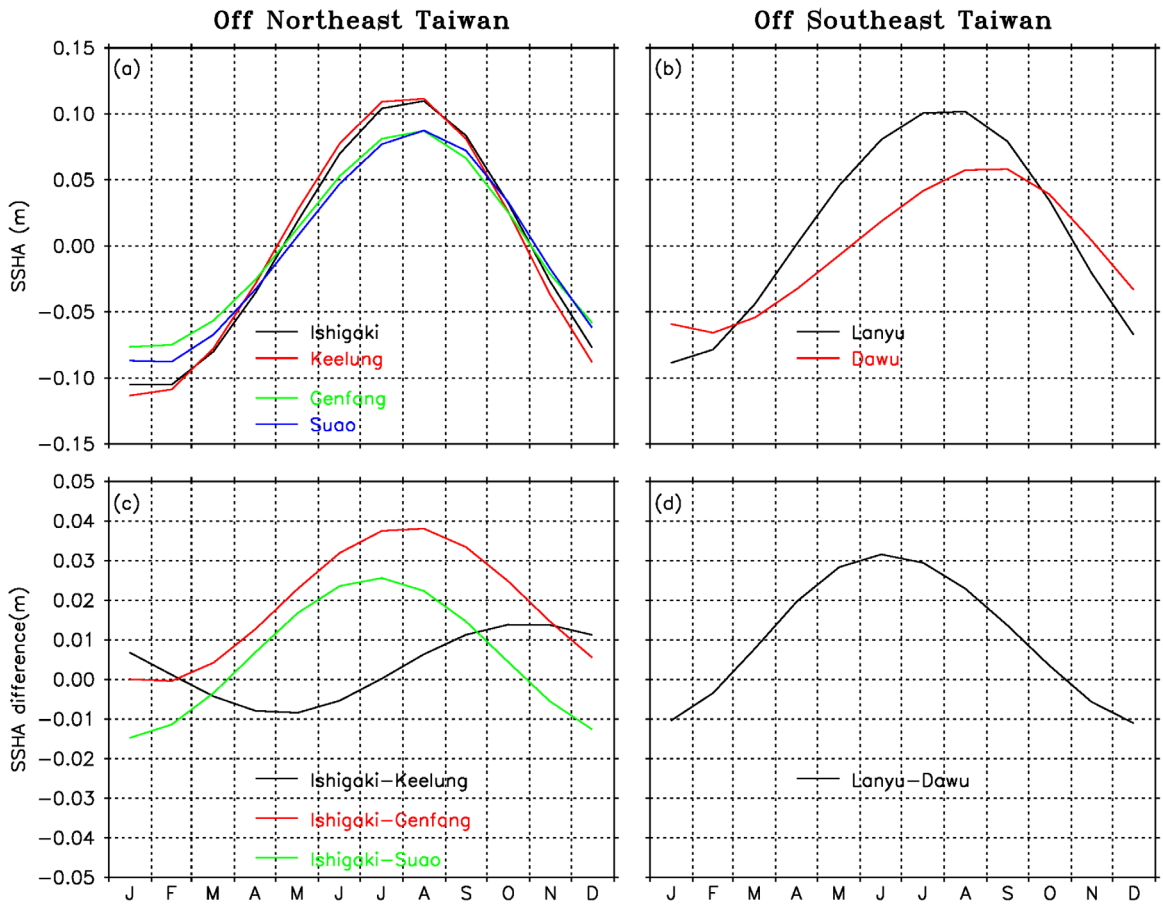

Figure 7. (top) Monthly distributions of sea level anomaly at six tidal-gauge stations and (bottom) sea level anomaly differences between the tidal-gauge station pairs. Left/right figures denote monthly distributions off northeast/southeast of Taiwan. Monthly values of tidal-gauge-derived sea level anomaly and the associated sea level anomaly difference are derived from the available data shown in Figure 2.

dominated by fluctuations on time scales shorter than 200 days. The meridional distributions of the explained variances of the INT_{Vg} on the intraseasonal and annual signals are similar to those of the KCP except that the explained variances of INT_{Vg} slightly decreased/increased on the intraseasonal/annual time scales. This outcome supports the previous studies that the mesoscale eddies strongly influence the Kuroshio east of Taiwan and lead to an insignificant annual variation [*Johns et al.*, 2001; *Hsin et al.*, 2008].

[18] The interannual variations only account for a small explained variance of less than 10%. With the Kuroshio flowing downstream, the explained variance of the interannual KCP increases from less than 5% in the south to larger than 5% in the north. On the contrary, the INT_{Vg} has an opposite northward-decreasing tendency of explained variance. The tendency of northward-increasing/decreasing explained variance of the interannual KCP/INT_{Vg} agrees well with the result of spectral analysis shown in Figure 4. Although the intraseasonal KCP and INT_{Vg} have large explained variances, their cause has been known to be related to the mesoscale eddies originating in the STCC. Thus, the fluctuations on this time scale will not be pursued in this study. In the following sections, we will focus our attention on the fluctuations of Kuroshio central position and intensity on the time scales longer than 200 days, i.e., seasonal and interannual.

[19] From our explained-variance analysis, it is worth noting that the seasonal fluctuation of the INT_{Vg} northeast of Taiwan is 5–10 times larger than the interannual one. This result disagrees with the argument proposed by *Chang and Oey* [2011] who showed that the seasonal fluctuation is 5–10 times weaker than the interannual fluctuations. This inconsistency is likely due to the differences in the calculation method and/or the data analyzed. *Chang and Oey* [2011] compared the amplitude of annual cycle of the tidal-gauge-derived SSHA difference with the fluctuations of the interannual tidal-gauge-derived SSHA difference time series, in which the annual cycle is removed. Thus, this interannual time series might still contain the intraseasonal fluctuations, which can dominate both the intensity and horizontal movement of the surface Kuroshio east of Taiwan (>70%, Figure 5), leading to the overestimation of the amplitude of interannual fluctuations of the tidal-gauge-derived Kuroshio transport.

3.3. Seasonality

[20] By averaging the 200–500 day band pass filtered KCP and INT_{Vg} month-by-month over the period of 1993–2012, we derive the monthly climatology of KCP and

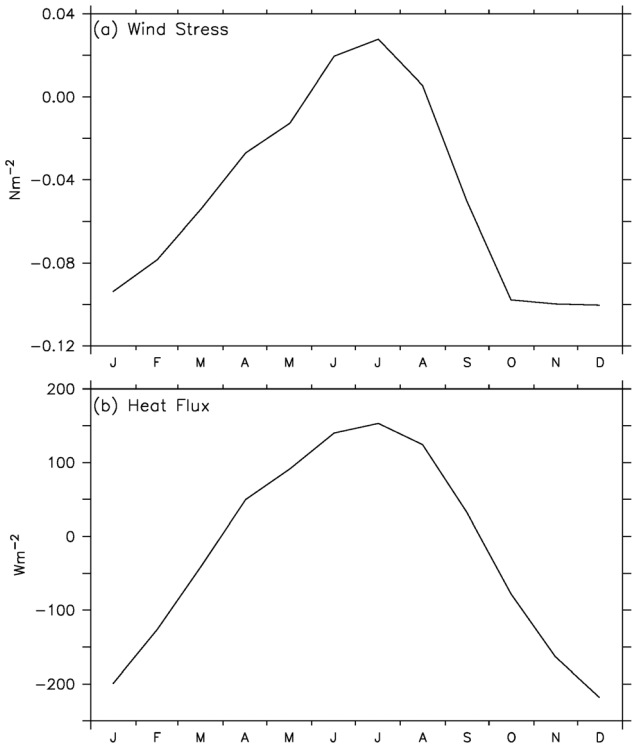

Figure 8. Monthly climatology of (a) along Kuroshio wind stress and (b) heat flux off northeast of Taiwan. Along Kuroshio wind stress is the wind stress component rotated at an angle of 70° parallel to the Kuroshio east of Taiwan. Wind stress and heat flux data are averaged over 121–122.5°E and 25.5–27°N. Monthly climatological wind stress is derived from the Cross-Calibrated Multi-Platform (CCMP) Ocean Surface Wind product [*Atlas et al*., 2008, 2009] in the period of 1988–2010. Monthly climatological net heat flux is derived from the reanalysis data of the Modern Era Retrospective-analysis for Research and Applications (MERRA; http://apdrc.soest.hawaii.edu).

INT_{Vg} in order to obtain the annual cycle of central position and intensity of the surface Kuroshio east of Taiwan. As shown in Figure 6, both KCP and INT_{Vg} have larger annual fluctuations in the northern and southern sections east of Taiwan. Comparing the annual cycles of KCP northeast versus southeast of Taiwan, they are nearly out of phase (Figure 6a). The KCP northeast of Taiwan is most offshore in August to September and most inshore in February to March. Southeast of Taiwan, the surface Kuroshio moves to the easternmost position in November to December and to the westernmost position in May to June.

[21] The intensity of surface Kuroshio east of Taiwan presents a uniform annual cycle with a maximum in July and a minimum in January (Figure 6b). Regarding the seasonal change of the Kuroshio intensity northeast of Taiwan, two different results were suggested in the literature: summer-winter (most of studies) versus fall-spring [*Chang and Oey*, 2011], while the annual cycle with a peak in summer and a trough in winter was proposed for the Kuroshio southeast of Taiwan [*Gilson and Roemmich*, 2002]. Northeast of Taiwan, our INT_{Vg} result supports most of the past studies, but differs from the recent finding by *Chang and Oey* [2011], who derived an annual cycle with a peak/trough in fall/spring from the 29 year tidal-gauge SSHA difference between Keelung and Ishigaki and ascribed this annual cycle to the seasonal variability of mesoscale eddies in the STCC area.

[22] To clarify the different annual cycle of Kuroshio intensity noted above, we compare the tidal-gauge-derived annual cycle of the Kuroshio intensity with the altimeter-derived result. Using the available monthly tidal-gauge-derived SSHA records, the monthly distributions of SSHA at the six stations are presented in Figures 7a and 7b. Except for the Dawu station where SSHA peaks in September and bottoms out in February, SSHA at the other five stations exhibit a uniform annual cycle with a maximum in July to August and a minimum in January to February. Figures 7c and 7d depict the monthly climatology of INT_{TG}, respectively, from the three station pairs northeast of Taiwan and one station pair southeast of Taiwan. Northeast of Taiwan, the annual cycle of INT_{TG} deviates among station pairs (Figure 7c). The INT_{TG} derived from station pairs of Ishigaki-Suao and Ishigaki-Genfang have a similar annual cycle with a minimum in January to February and a maximum in July to August; however, that derived from station pair of Ishigaki-Keelung shows an obviously different annual cycle with a peak in October to November and a trough in April to May, which is consistent with the annual cycle found by *Chang and Oey* [2011] and has been regarded to be associated with mesoscale eddies in the STCC area. The outcome of this study shows that the impinging mesoscale eddies from the STCC area are not the cause for generating the fall-spring annual cycle of SSHA difference between Keelung and Ishigaki. Rather, the Keelung station is located over the southern ECS shelf where SSHAs are perturbed by monsoonal winds, seasonal heating/cooling, and other oceanic perturbations over the ECS shelf, and it may not constitute an ideal station for estimating the seasonal Kuroshio transport variation east of Taiwan. Regarding the INT_{TG} southeast of Taiwan, the surface Kuroshio strengthens in June to July and weakens in December to January (Figure 7d), showing an annual cycle consistent with the satellite-altimeter-derived Kuroshio intensity (INT_{Vg}; Figure 6b).

[23] In summary, the surface Kuroshio east of Taiwan is strongest in summer and weakest in winter; the center of Kuroshio southeast of Taiwan is closest/farthest to Taiwan in summer/winter, while northeast of Taiwan, it has a closest/farthest position to the coast in winter/summer. In terms of the seasonal movement of the Kuroshio northeast of Taiwan, two possible dynamic explanations have been proposed in the literature. One is the Ekman dynamical explanation with a time scale of shorter than 1 month [*Chao*, 1991] and the other is the Joint Effect of Baroclinic and Relief (JEBAR) related to the surface heating/cooling northeast of Taiwan with a time scale of 1–2 months [e.g., *Chuang and Liang*, 1994; *Oey et al*., 2010]. As shown in Figure 8, the wind stress and net heat flux northeast of Taiwan reach the seasonal maxima/minima in December to January/July. Such a seasonal forcing indicates that our satellite-altimeter-derived KCP northeast of Taiwan supports the JEBAR explanation because the extreme values of the monsoonal winds and heat fluxes around the southern ECS shelf take place 1–2 months prior to the peaking month of KCP.

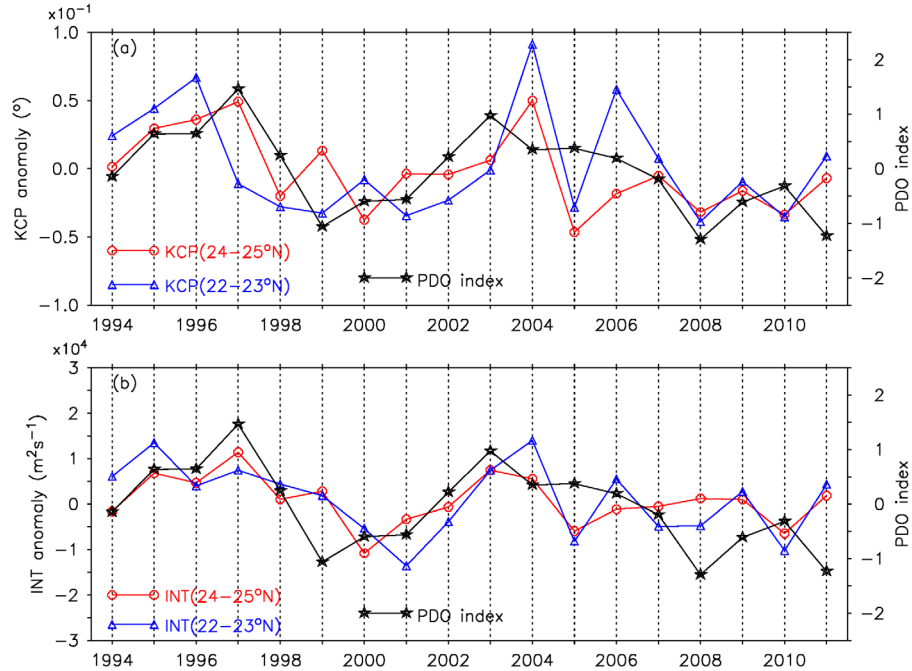

Figure 9. Yearly averaged anomalies of Kuroshio (a) central position and (b) intensity off northeast of Taiwan (24–25°N; red line with circle) and southeast of Taiwan (22–23°N; blue line with triangle) with superposed by the yearly averaged PDO index (black line with star). The yearly anomalies are averaged annually from the 500 day low pass filtered time series.

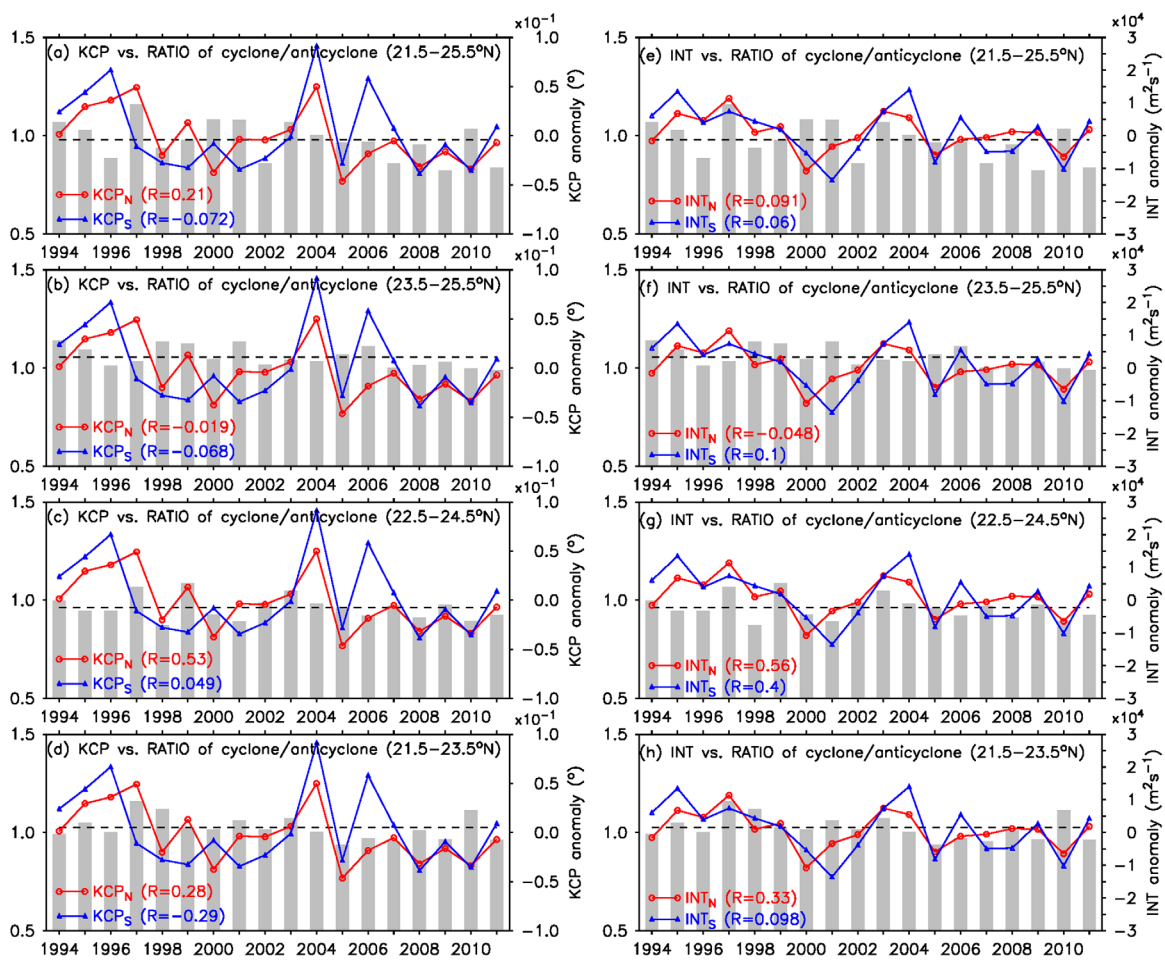

Figure 10. Ratio of yearly averaged number of cyclonic to anticyclonic eddies between 125 and 126°E (gray bars) superposed by yearly anomalies of Kuroshio central position (left) and intensity (right). Correlation coefficients between the ratio and central position/intensity are labeled. Black dashed line denotes the average of ratio.

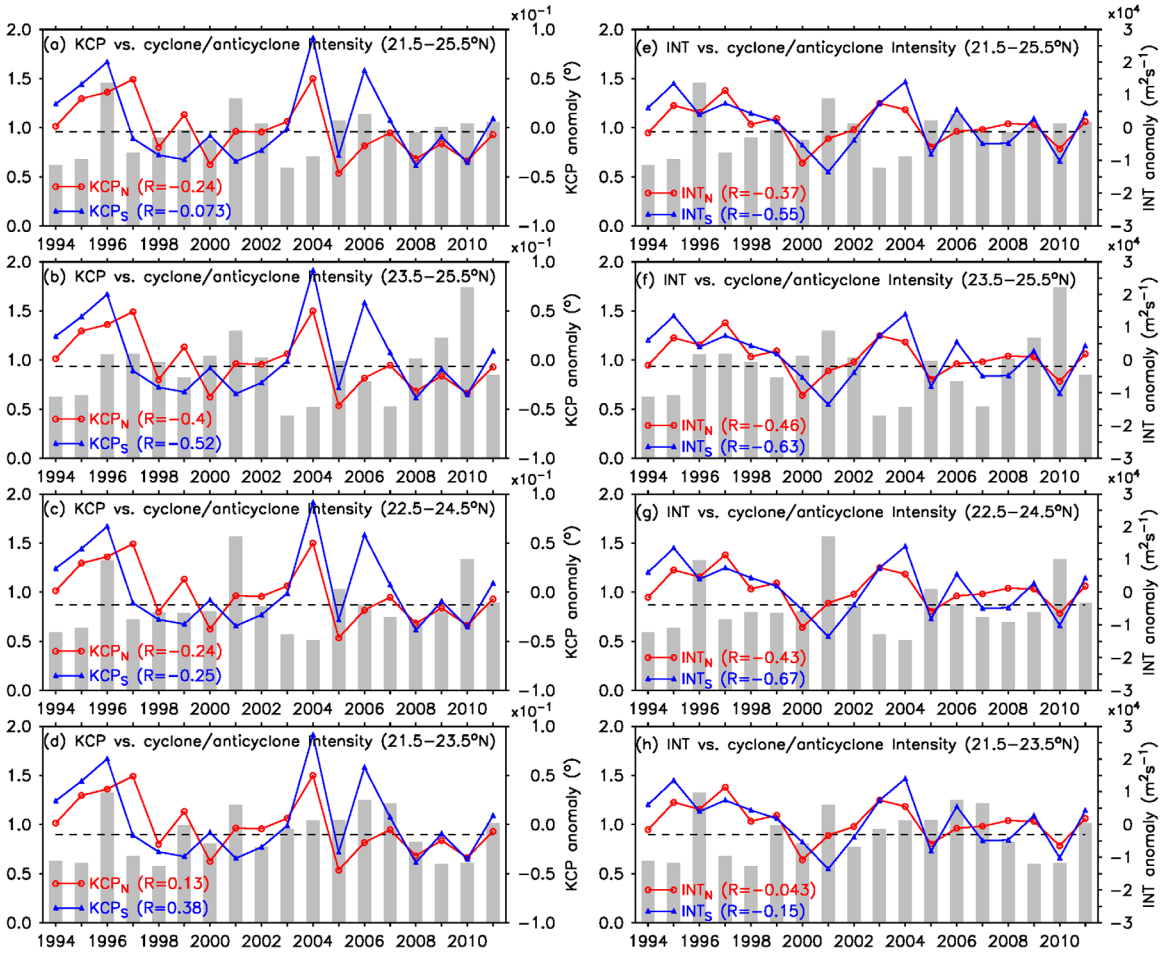

Figure 11. Same as Figure 10, but for the yearly averaged ratio of the cyclonic eddy's intensity to anticyclonic eddy's intensity. The eddy's intensity is defined as the absolute vorticity on the center of eddies.

[24] As to the KCP southeast of Taiwan, the Kuroshio moves to the most inshore position in May to June and to the most offshore one in November to December. *Hsin et al*. [2010] found a high correlation between the changes of the meridional velocity (V) southeast of Taiwan and the zonal velocity (U) in the northern part of the Luzon Strait, and suggested the inertial effect of this zonal current to be the cause. On the other hand, the upper-layer transport through the Luzon Strait has a clear annual cycle with a maximum westward transport in December and a minimum in June [*Qu*, 2000; *Hsin and Qiu*, 2012]. Moreover, the Kuroshio transport east of the Luzon Island reaches the largest and smallest value in May and October, respectively [*Qiu and Lukas*, 1996]. Therefore, the combined effect of the Kuroshio transport east of the Luzon Island and in the Luzon Strait can likely regulate the Kuroshio central position southeast of Taiwan. Specifically, during winter the large loop current occurs inside the Luzon Strait that can lead to a larger eastward current in the northern Luzon Strait and generate, in turn, an offshore movement of Kuroshio center off southeast of Taiwan because of inertia. Similarly, the Kuroshio southeast of Taiwan moves inshore in summer when the upstream Kuroshio in the Luzon Strait is stronger and tends to have a relatively straight path.

3.4. Interannual Variability

[25] As mentioned in section 1, interannual changes of the Kuroshio transport (i.e., intensity) east of Taiwan have been described in the literature [*Gilson and Roemmich*, 2002; *Hwang and Kao*, 2002; *Chang and Oey*, 2011]. However, there are, to date, no studies describing the interannual changes of the Kuroshio central position in this area. The yearly averaged 500 day low pass filtered time series are used in this section to investigate the interannual changes of the Kuroshio central position and intensity (Figure 9). In addition, the yearly averaged KCP and INT_{Vg} anomalies are averaged over 22–23°N and 24–25°N in order to compare the interannual changes of the Kuroshio off the northeast versus southeast of Taiwan.

[26] During 1993–2012, the KCP and INT_{Vg} northeast of Taiwan have concurrent changes with those southeast of Taiwan (Figure 9). The correlation coefficient (R) between KCP (INT_{Vg}) northeast and southeast of Taiwan is 0.59 (0.76). In general, the Kuroshio extends to a more offshore position during 1995–1997 and 2004–2007 when its strength reaches a higher level. The correlation coefficients of KCP and INT_{Vg} are 0.82 and 0.69 for the northeast and southeast of Taiwan, respectively. This outcome indicates

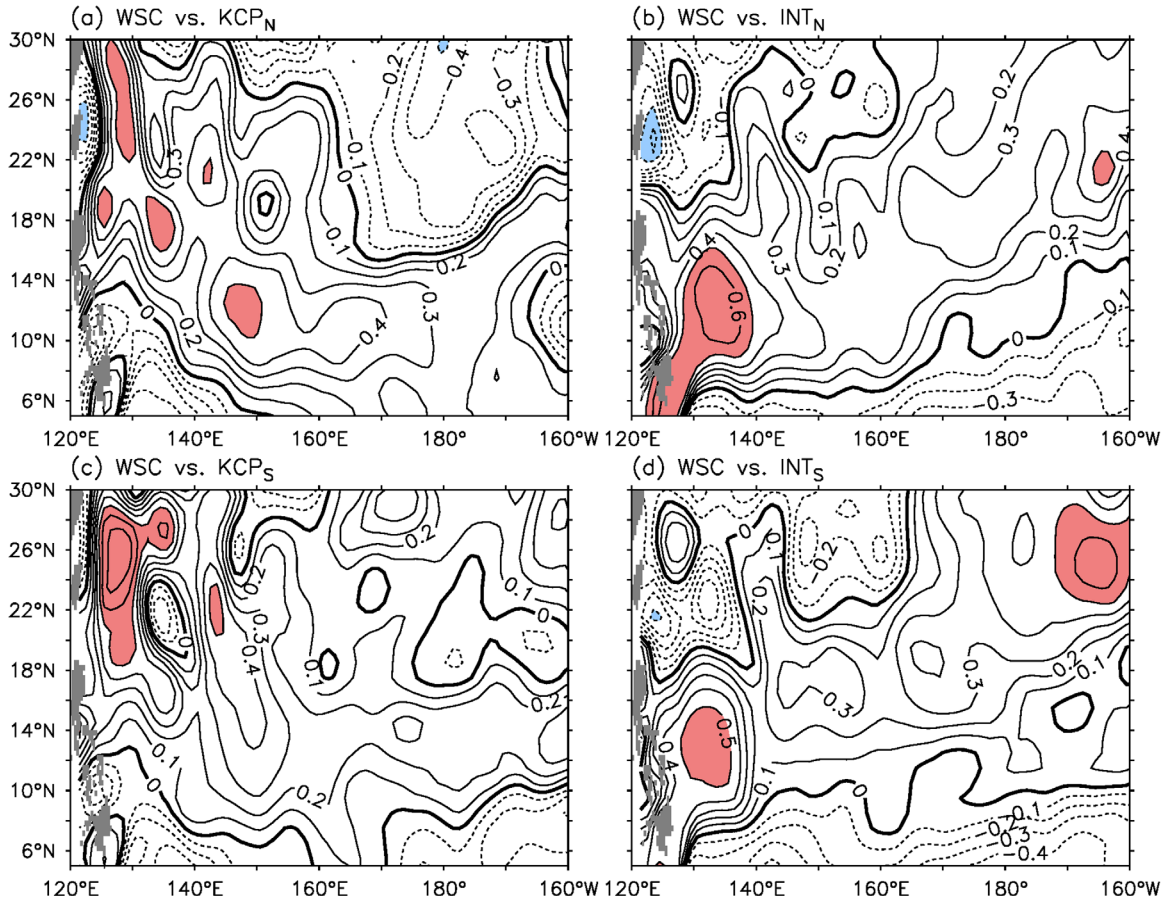

Figure 12. Correlation coefficients of 500–1500 day band pass filtered wind stress curl (WSC) and Kuroshio central position (KCP, left) and intensity (INT_{Vg}, bottom) (top) off northeast and (bottom) southeast of Taiwan. Shading with red (blue) color labels the area with correlation coefficient greater (less) than 0.5 (−0.5).

that KCP and INT_{Vg} throughout the eastern Taiwan have nearly simultaneous interannual changes.

[27] The timing of the INT_{Vg} and KCP peaks agrees very well with the warm phase (1996–1998 and 2003–2006) of the PDO index and also the high level of decadal STCC eddy kinetic energy (EKE) index [*Qiu and Chen*, 2010, 2013], showing that the eddy activities in the STCC band enhanced in 1995–1998 and 2003–2006 and weakened in 1999–2002 and 2009–2011. *Qiu and Chen* [2010] found that the enhanced eddy activities are caused by the enhanced baroclinic instability resulting from the larger vertical shear of zonal velocity in the STCC-NEC's background flow. *Qiu and Chen* [2013] further ascribed this velocity shear change to the decadally varying surface heat flux forcing. Our result of Figure 9 indicates that the decadal change of Kuroshio east of Taiwan could be relevant to the PDO-related eddy activities in the STCC band. On the other hand, *Chang and Oey* [2012] also suggested that the larger Kuroshio transport between Keelung and Ishigaki is induced by the high EKE in the STCC area. To further explore why a high level of EKE can intensify the Kuroshio, it is of interest to quantify whether the amount of eddies approaching east of Taiwan (125–126°E, 21.5–25.5°N) is related to the Kuroshio variations (INT_{Vg} or KCP). To answer this question, we count the amount of eddies by finding the maximal or minimal value of relative vorticity $\left(\xi = \partial V_g/\partial x - \partial U_g/\partial y\right)$ derived from the altimeter-based geostrophic velocity. In the northern hemisphere, positive vorticity denotes the presence of a cyclonic eddy, whereas negative vorticity, an anticyclonic eddy.

[28] When comparing the year-to-year change of total eddy number with the PDO index, the decadal STCC EKE index, KCP, or INT_{Vg}, we find no good correlations (correlation coefficient <0.4, figure not shown). This result indicates that the amount of eddies impinging upon the eastern Taiwan could not be directly responsible for the interannual changes of Kuroshio central position and intensity. *Yang et al*. [1999] detected that, on the intraseasonal time scales (70–200 days), the impinging of an anticyclonic (cyclonic) eddy can lead to an increase (decrease) in the Kuroshio transport through the ETC by deforming the Kuroshio path east of Taiwan. Thus, we hypothesize that a larger (smaller) Kuroshio transport may take place in years when more anticyclonic (cyclonic) eddies impinging upon the east of Taiwan. To test this hypothesis, the amounts of cyclonic versus anticyclonic eddies are further inspected by calculating the ratio of the cyclonic to the anticyclonic eddies. When the ratio is greater (less) than one, more cyclonic (anticyclone) eddies impinge upon the area studied.

[29] As shown in Figure 10, there are, on average, more anticyclonic eddies impinging in the area between 21.5 and

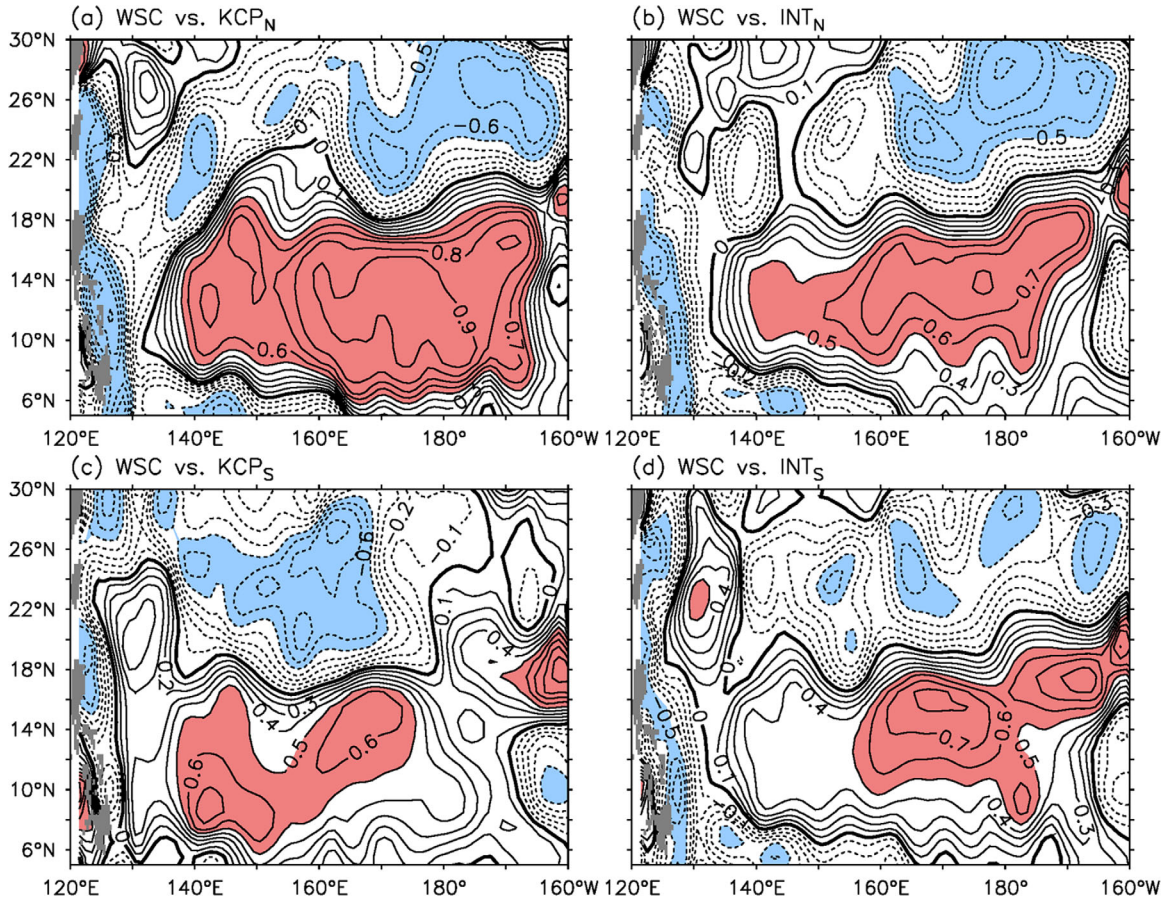

Figure 13. Same as Figure 12, but for the 1500 day low pass filtered wind stress curl and Kuroshio central position and intensity.

25.5°N, whereas there are more cyclonic eddies impinging in the northern section (23.5–25.5°N). Moreover, the ratio of cyclonic to anticyclonic eddies undergoes a strong interannual change, and this interannual change differs among areas. For example, more anticyclonic eddies exist in the northern and southern sections east of Taiwan (Figures 10b and 10d) but less in the middle section (Figure 10c). The correlation coefficients are not obviously improved (compared to the total eddy number), when the cyclonic and anticyclonic eddies are separately considered, implying that the relative number of cyclonic versus anticyclonic eddies is also not a direct cause to the interannual Kuroshio changes.

[30] To further take the intensity of cyclonic/anticyclonic eddy into consideration, we examine the yearly averaged ratio of cyclonic to anticyclonic eddy's intensity (Figure 11). The correlation coefficients are significantly improved in 23.5–25.5°N for both the KCP (Figure 11b) and INT_{Vg} (Figures 11f) through the whole eastern Taiwan. This outcome suggests that the relative intensity of cyclonic versus anticyclonic eddies in 23.5–25.5°N is likely one of the major causes in modulating the interannual changes of both the Kuroshio intensity and central position. Moreover, the relative intensity of eddies in 22.5–25.5°N has a more significant effect on the interannual changes of the Kuroshio than that in 21.5–23.5°N.

[31] Except for the impact of eddies, wind forcing is also thought of as one of the factors in altering the interannual changes of the Kuroshio [e.g., *Akitomo et al.*, 1996; *Qiu and Lukas*, 1996; *Deser et al.*, 1999; *Qiu and Chen*, 2005; *Chang and Oey*, 2012]. To explore the effect of wind forcing on the Kuroshio east of Taiwan on the interannual and decadal time scales, we plot in Figures 12 (Figure 13) the correlation coefficients between the 500–1500 day band pass filtered (1500 day low-pass filtered) wind stress curl (WSC) data and the KCP/INT_{Vg} data (left/right figures) off northeast/southeast of Taiwan (upper/lower figures). As shown in Figure 12, on the time scales shorter than 1500 days (about 4 years), KCP off the whole eastern Taiwan has a higher positive R with WSC east of 130°E off eastern Taiwan, whereas INT_{Vg} off the whole eastern Taiwan has a higher negative (positive) R with WSC west of 140°E off eastern Taiwan (Philippines). On the longer time scale (Figure 13, >1500 days), both KCP and INT_{Vg} off the whole eastern Taiwan are positively correlated with WSC east of about 135°E and south of 18°N, but negatively with WSC east of 140°E and north of 20°N.

[32] To sum up, the 500–1500 day fluctuations of INT_{Vg} are related to the local WSC dipole (west of 140°E) near the eastern coasts of Taiwan and the Philippines, whereas the INT_{Vg} and KCP on the time scale longer than 1500 days have better connections with the larger-scale WSC dipole east of 140°E and are also influenced by the local WSC along the coasts of Taiwan and the Philippines. Besides, the KCP and INT_{Vg} are negatively correlated with WSC near the coasts from the Philippines to Taiwan.

4. Concluding Remarks

[33] A 20 year (1993–2012) altimetry product is adopted in this study to explore the seasonal and interannual changes in the intensity and central position of the Kuroshio east of Taiwan. Seasonally, the Kuroshio throughout the eastern coast of Taiwan strengthens in summer and weakens in winter. However, the Kuroshio position changes nonuniformly along the coast: it moves offshore (inshore) off southeast (northeast) of Taiwan in winter. The seasonal movement of the Kuroshio off northeast of Taiwan is caused by seasonal heating/cooling over the ECS shelf, whereas off southeast of Taiwan it is due to the combined effect of the upstream Kuroshio transport through the Luzon Strait and the eastern Luzon Island.

[34] On the interannual time scales, the Kuroshio throughout the eastern Taiwan intensifies with a more offshore path during the periods of 1995–1997 and 2004–2007 when the PDO index is in the warm phase and the PDO-related STCC EKE index reaches a high level. By examining the (relative) number and intensity of eddies impinging upon the eastern coast of Taiwan, we detect the relative intensity of cyclonic versus anticyclonic eddies in 22.5–25.5°N to be one of the major causes in modulating the interannual changes of the Kuroshio central position and intensity. Specifically, the surface Kuroshio throughout the eastern Taiwan tends to be intensified (weakened) and have a more offshore (inshore) path in years when the anticyclonic (cyclonic) eddies off eastern Taiwan intensify relatively.

[35] **Acknowledgments.** This research was financially supported by the Taiwan National Science Council grants NSC 102-2611-M-001-001-MY2 and 101-2811-M-003–017. Y.C.H. and B.Q. also acknowledge the support by the ONR project Origins of the Kuroshio and Mindanao Current, N00014-10-1-0267.

References

Akitomo, K., M. Ooi, T. Awaji, and K. Kutsuwada (1996), Interannual variability of the Kuroshio transport in response to the wind stress field over the North Pacific: Its relation to the path variation south of Japan, *J. Geophys. Res.*, *101*(C6), 14,057–14,071, doi:10.1029/96JC01000.

Atlas, R., J. Ardizzone, and R. N. Hoffman (2008), Application of satellite surface wind data to ocean wind analysis, *Proc. SPIE*, *7087*, 70870B, doi:10.1117/12.795371.

Atlas, R., R. N. Hoffman, J. Ardizzone, S. M. Leidner, and J. C. Jusem (2009), Development of a new cross-calibrated, multi-platform (CCMP) ocean surface wind product, in *AMS 13th Conference on Integrated Observing and Assimilation Systems for Atmosphere, Oceans, and Land Surface*, Phoenix, Arizona.

Chang, Y.-L., and L.-Y. Oey (2011), Interannual and seasonal variations of Kuroshio transport east of Taiwan inferred from 29 years of tide-gauge data, *Geophys. Res. Lett.*, *38*, L08603, doi:10.1029/2011GL047062.

Chang, Y.-L., and L.-Y. Oey (2012), The Philippines-Taiwan Oscillation: Monsoonlike interannual oscillation of the subtropical-tropical western north Pacific wind system and its impact on the ocean, *J. Clim.*, *25*, 1597–1618, doi:10.1175/JCLI-D-11-00158.1.

Chao, S.-Y. (1991), Circulation of the East China Sea, a numerical study, *J. Oceanogr.*, *42*, 273–295, doi:10.1007/BF02123503.

Chen, C.-T. A. (1996), The Kuroshio intermediate water is the major source of nutrients on the East China Sea continental shelf, *Oceanol. Acta*, *19*, 523–527.

Chuang, W.-S., and W.-D. Liang (1994), Seasonal variability of intrusion of the Kuroshio water across the continental shelf northeast of Taiwan, *J. Oceanogr.*, *50*, 531–542, doi:10.1007/BF02235422.

Deser, C., M. A. Alexander, and M. S. Timlin (1999), Evidence for a wind-driven intensification of the Kuroshio current extension from the 1970s to the 1980s, *J. Clim.*, *12*, 1697–1706, doi:10.1175/1520-0442(1999)012<1697:EFAWDI>2.0.CO;2.

Gilson, J., and D. Roemmich (2002), Mean and temporal variability of Kuroshio geostrophic transport south of Taiwan (1993–2001), *J. Oceanogr.*, *58*, 183–195, doi:10.1023/A:1015841120927.

Hsin, Y.-C., and B. Qiu (2012), Seasonal fluctuations of the surface North Equatorial Countercurrent (NECC) across the Pacific basin, *J. Geophys. Res.*, *117*, C06001, doi:10.1029/2011JC007794.

Hsin, Y.-C., C.-R. Wu, and P.-T. Shaw (2008), Spatial and temporal variations of the Kuroshio east of Taiwan, 1982–2005: A numerical study, *J. Geophys. Res.*, *113*, C04002, doi:10.1029/2007JC004485.

Hsin, Y.-C., T. Qu, and C.-R. Wu (2010), Intra-seasonal variation of the Kuroshio southeast of Taiwan and its possible forcing mechanism, *Ocean Dyn.*, *60*, 1293–1306, doi:10.1007/s10236-010-0294-2.

Hsin, Y.-C., T.-L. Chiang, and C.-R. Wu (2011), Fluctuations of the thermal fronts off northeastern Taiwan, *J. Geophys. Res.*, *116*, C10005, doi:10.1029/2011JC007066.

Hwang, C., and R. Kao (2002), TOPEX/POSEIDON-derived space-time variations of the Kuroshio Current: Applications of a gravimetric geoid and wavelet analysis, *Geophys. J. Int.*, *151*, 835–847, doi:10.1046/j.1365-246X.2002.01811.x.

Hwang, C., C.-R. Wu, and R. Kao (2004), TOPEX/Poseidon observations of mesoscale eddies over the Subtropical Countercurrent: Kinematic characteristics of an anticyclonic eddy and a cyclonic eddy, *J. Geophys. Res.*, *109*, C08013, doi:10.1029/2003JC002026.

Ichikawa, K., R. Tokeshi, M. Kashima, K. Sato, T. Matsuoka, S. Kojima, and S. Fujii (2008), Kuroshio variations in the upstream region as seen by HF radar and satellite altimetry data, *Int. J. Remote Sens.*, *29*(21), 6417–6426, doi:10.1080/01431160802175454.

Johns, W. E., T. N. Lee, D. Zhang, R. Zantopp, C.-T. Liu, and Y. Yang (2001), The Kuroshio east of Taiwan: Moored transport observations from the WOCE PCM-1 array, *J. Phys. Oceanogr.*, *31*, 1031–1053, doi:10.1175/1520-0485(2001)031<1031:TKEOTM>2.0.CO;2.

Liang, W.-D., T. Y. Tang, Y. J. Yang, M. T. Ko, and W.-S. Chuang (2003), Upper-ocean currents around Taiwan, *Deep Sea Res., Part II*, *50*, 1085–1105, doi:10.1016/S0967-0645(03)00011-0.

Oey, L.-Y., Y.-C. Hsin, and C.-R. Wu (2010), Why does the Kuroshio northeast of Taiwan shift shelfward in winter?, *Ocean Dyn.*, *60*, 413–426, doi:10.1007/s10236-009-0259-5.

Qiu, B. (1999), Seasonal eddy field modulation of the north Pacific STCC: TOPEX/Poseidon observations and theory, *J. Phys. Oceanogr.*, *29*, 2471–2486, doi:10.1175/1520-0485(1999)029<2471:SEFMOT>2.0.CO;2.

Qiu, B., and S. Chen (2005), Variability of the Kuroshio extension jet, recirculation gyre, and mesoscale eddies on decadal time scales, *J. Phys. Oceanogr.*, *35*, 2090–2103, doi:10.1175/JPO2807.1.

Qiu, B., and S. Chen (2010), Interannual variability of the North Pacific subtropical countercurrent and its associated mesoscale eddy field, *J. Phys. Oceanogr.*, *40*, 213–225, doi:10.1175/2009JPO4285.1.

Qiu, B., and S. Chen (2013), Concurrent decadal mesoscale eddy modulations in the western North Pacific subtropical gyre, *J. Phys. Oceanogr.*, *43*, 344–358, doi:10.1175/JPO-D-12–0133.1.

Qiu, B., and R. Lukas (1996), Seasonal and interannual variability of the North Equatorial Current, the Mindanao Current, and the Kuroshio along the Pacific western boundary, *J. Geophys. Res.*, *101*, 12,315–12,330, doi:10.1029/95JC03204.

Qu, T. (2000), Upper-layer circulation in the South China Sea, *J. Phys. Oceanogr.*, *30*, 1450–1460, doi:10.1175/1520-0485(2000)030<1450:ULCITS>2.0.CO;2.

Rio, M. H., S. Guinehut, and G. Larnicol (2011), New CNES-CLS09 global mean dynamic topography computed from the combination of GRACE data, altimetry, and in situ measurements, *J. Geophys. Res.*, *116*, C07018, doi:10.1029/2010JC006505.

Sun, X. (1987), *Analysis of the surface path of the Kuroshio in the East China Sea, in Essays on Investigation of Kuroshio*, edited by X. Sun, pp. 1–14, China Ocean Press, Beijing.

Tang, T. Y., and Y.-J. Yang (1993), Low frequency current variability on the shelf break northeast of Taiwan, *J. Oceanogr.*, *49*(19), 193–210, doi:10.1007/BF02237288.

Wu, C.-R. (2013), Interannual modulation of the Pacific Decadal Oscillation (PDO) on the low-latitude western North Pacific, *Prog. Oceanogr.*, *110*, 49–58, doi:10.1016/j.pocean.2012.12.001.

Yang, Y., C.-T. Liu, J.-H. Hu, and M. Koga (1999), Taiwan Current (Kuroshio) and impinging eddies, *J. Oceanogr.*, *55*, 609–617, doi:10.1023/A:1007892819134.

Yang, Y., C.-T. Liu, T. N. Lee, W. Johns, H.-W. Li, and M. Koga (2001), Sea surface slope as an estimator the Kuroshio volume transport east of Taiwan, *Geophys. Res. Lett.*, *28*(12), 2461–2464, doi:10.1029/2000GL011709.